Fronthaul Signal Compression in C-RAN with Carrier Aggregation

Marcos Takeda, Leonardo Ramalho, Chenguang Lu, Miguel Berg and Aldebaro Klautau

***Abstract*— Cloud-radio access networks (C-RAN) and carrier aggregation are enabling technologies for high data rate in mobile communications. However, a drawback of C-RAN is the high volume of data that must be transmitted between the baseband unit (BBU) and the remote radio head (RRH). Moreover, this amount of data increases linearly with the number of components carriers that are used in carrier aggregation. Fronthaul signal compression can reduce this huge volume of data, but the available compression schemes have been tested only with LTE signals, not taking into consideration specific characteristics of carrier aggregation. This paper provides an overview of important aspects of carrier aggregation signals that are relevant for the compression of these signals in C-RAN, and discusses simulation results in different scenarios.**

***Keywords*— Fronthaul, C-RAN, Carrier Aggregation, LPC.**

I. INTRODUCTION

Mobile networks are evolving to provide higher throughput, lower latency and better user experience while keeping the network costs affordable for operators. In this context, Cloud-Radio Access Network (C-RAN) is a novel radio network architecture that can address these requirements. C-RAN is able to provide better signal coverage, increased cells density and lower the costs for installing new radio cells [1].

In C-RAN, the operations of a radio base station are executed by two units, called baseband unit (BBU) and remote radio head (RRH). The former performs all the baseband signal processing while the latter is responsible for both baseband-RF conversion and RF transmission and reception. The digital complex representation of the baseband signal is transported between the BBU and RRH through a high-speed link named fronthaul. To decrease the fronthaul bit rate, distinct functionality splits have been considered for 5G networks [2], but here the scope is restricted to fronthauls transmitting IQ samples.

The transmission of the IQ samples between the BBU and RRH requires a high transmission rate in the fronthaul. However, this rate can be reduced with fronthaul signal compression (FSC), which decreases the volume of data to represent the radio signal before transporting the baseband complex signals over the fronthaul [3]–[7].

This work was supported in part by the EU H2020 5G-CORAL Project (grant no. 761586), the Innovation Center, Ericsson Telecomunicações S.A., Brazil, CNPq and the Capes Foundation, Ministry of Education of Brazil.

Marcos Takeda, Aldebaro Klautau are with Computer and Telecommunications Engineering Department at Federal University of Para, Belem 66615-170, Brazil. E-mails: marcos.takeda@itec.ufpa.br and aldebaro@ufpa.br.

Leonardo Ramalho is with Federal Institute of Para, Belem 66093-020, Brazil. Email: leonardo.ramalho@ifpa.edu.br

Chenguang Lu and Miguel Berg are with Ericsson Research, 164 80 Kista, Sweden. Emails: chenguang.lu@ericsson.com and miguel.berg@ericsson.com

In addition to C-RAN, carrier aggregation (CA) is another enabling technology that can improve cell capacity by extending the available radio bandwidth [8]. For example, LTE-Advanced (LTE-A) can provide peak data rates of 1 Gb/s and 500 Mb/s in downlink and uplink by incorporating CA with other technologies in physical layer, such as multiple-input multiple-output (MIMO) and orthogonal frequency division multiplexing (OFDM) [9]. MIMO and OFDM were already present on LTE Release 8/9, but CA was introduced in 3GPP Release 10 specification which is commonly known as LTE-A.

In LTE-A, carrier aggregation combines up to five portions of spectrum, called component carriers (CC), where each CC is backward compatible with LTE Release 8/9. Thus, a LTE-A user might use up to 100 MHz of spectrum, and at the same time legacy users can use the spectrum of each CC, independently [10].

Basically, there are three types of spectrum configuration for carrier aggregation [8]: interband, intraband noncontiguous and intraband contiguous. Fig. 1 shows these three scenarios with two components carriers. In interband spectrum scenario, the physical signals of each CC are created similarly to LTE release 8/9 signals. On the other hand, for intraband CA, the baseband signals for each CC are multiplexed into a wider band [11]–[13], and then this signal is upconverted and transmitted through a wideband RF frontend.

In interband configuration the digital baseband signal of each CC is created independently. Thus, in a C-RAN deployment the fronthaul could also transport each CC signal between BBU and RRH, separately. In these cases, a variety of FSC schemes could be used to compress each CC individually. Since these signals are similar to legacy LTE signals [14], the available FSC schemes (e. g., [3]–[7]) would work with these CA signals without extra adaptations.

However, for intraband CA signals, some available FSC schemes might not properly work, because in some cases these signals could have a different structure from the legacy LTE signals. A very important characteristic of the non-CA LTE signals is the oversampling factor, given by OSR $= \frac{F_s/2}{f_{\mathrm{MAX}}} \approx 1.7$, where F_s is the sampling frequency and f_{MAX} is the highest subcarrier frequency that can be used. The OSR is largely exploited by FSC schemes that are based on resampling [4]–[6], but the oversampling ratio of an intraband CA signals may vary depending on the the desired center frequency of each component carrier.

This paper shows spectrum aspects of intraband CA signals that are relevant for FSC schemes, such as OSR and the position of each CC. Moreover, the paper evaluates two options for compression of intraband CA signals: compression of each

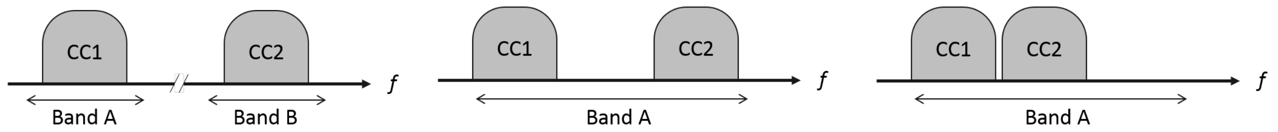

(a) Interband CA. (b) Intraband CA in noncontiguous mode. (c) Intraband CA in contiguous mode.

Fig. 1: Spectrum scenarios in carrier aggregation deployments.

CC independently and compression of a single intraband CA signal. Another contribution of this paper is to show that the FSC method previously proposed by the authors in [3] can be conveniently applied to intraband CA signals.

The remaining of this paper is organized as follows. Section II shows some characteristics of CA signals and aspects related to the compression of these signals. Section III shows the simulations results for compression of CA signals in different scenarios, while Section IV presents the final considerations.

II. Signal Model and Fronthaul Signal Compression

In this work, we create a baseband CA signal by generating each baseband CC signal, independently, and then, using a combination of upsampling and frequency shift. The upsampling allows to move the center frequency of each baseband CC signal to a frequency $f_c \neq 0$ and the shift in the frequency can be implemented by multiplying the resampled signal by a complex exponential $e^{j\omega_c n}$, where n is the discrete time-index and ω_c is the desired center angular frequency, given by $\omega_c = \frac{2\pi f_c}{F_s}$. Finally, The CA signal is obtained in this case by summing all resampled and frequency-shifted versions of each component carrier signal.

Independently on how the CA signal is created, the spacing between the center frequencies (ΔF_c) of each CC must be multiple of 300 kHz, to satisfy the LTE channel raster (100 kHz) and the subcarrier spacing (15 kHz) [8], [11]. In LTE deployments without CA, the baseband digital signal is created with $\omega_c = 0$, as shown in Fig. 2a. In these cases of non-CA signals, the RF center frequency (F_c) can be defined by a local oscillator with frequency F_{LO}. On the other hand, for CA deployments that the CA signal is represented by a single digital baseband signal, the RF center frequency of a given component carrier is also modified by its baseband center frequency f_c, i. e., $F_c = f_c + F_{LO}$.

The value of the baseband center frequency f_c might changes the value of f_{MAX} in a given CA signal. For example, assuming an intraband CA signal composed of two 20-MHz component carriers that use all available resource blocks (RB), Fig. 2b and 2c show two possible spectrum arrangements for the baseband CA signal. In both cases, the CA signal is sampled with $F_s = 61.44$ MHz and the center frequencies are spaced by 19.8 and 38.6 MHz in Fig. 2b and 2c, respectively.

In Fig. 2b, the sampling rate is $F_s = 61.44$ MHz and the OSR is approximately 1.63. The required fronthaul rate to transport this CA signal for a single antenna would be 1.84 Gbps, assuming that each time-domain complex sample is represented with 30 bits. Fronthaul signal compression can be applied to these CA signals, in order to decrease the required fronthaul rate. Resampling is a common technique used in many FSC schemes (see, e. g., [4]–[6]), which basically decreases the number of samples by downsampling the signal and not transmitting unused high frequencies. The spectrum of the CA signal in Fig. 2b is similar to the non-CA LTE signal in Fig. 2a, as shown by the angular frequency. In these cases, approximately 1/3 of the bandwidth is not used and can be discarded to transport the signal over the fronthaul and recovered at the decompression, as proposed in [4]–[6]. Furthermore, other FSC schemes [3], [7] also have good performance for the signals of Fig. 2b.

Nevertheless, the CA signal could have a spectrum arrangement that is different from a non-CA LTE signal, as shown in Fig. 2c. In this case the required fronthaul rate is also 1.84 Gbps, since the only difference from Fig. 2b is the position of the CCs, i. e., the sampling frequency is 61.44 MHz and each uncompressed complex sample is represented with 30 bits. However, FSC schemes that rely on resampling cannot be directly applied, because the maximum frequency used is close to the Nyquist frequency. Thus, other FSC methods should be evaluated to CA deployments that have baseband spectrum distinct from LTE signals.

The position of each CC in a intraband CA signal might be problematic for some FSC schemes, as detailed above. One way of circumventing this problem is to compress each CC independently, transmit them through the fronthaul and then at RRH the intraband CA signal is created by resampling and shifting to the desired center frequency f_c. Fig 3a shows this procedure for two CCs, where CCG stands for component carrier generation and FSC is the implemented frothaul signal compression. At the RRH, each CC is decompressed (in the FSD, fronthaul signal decompression) and the signals are upsampled by M and centered at the desired frequency w_c. Finally, the desired intraband CA signal $\hat{s}_{CA}$ is the sum of the resampled and shifted signals.

The intraband CA signal that contains more than one component carrier can be also compressed, as shown in Fig. 3b, where $s_{CA}[n]$ and $\hat{s}_{CA}[n]$ are the time-domain complex intraband CA signals before compression and after decompression, respectively. However, the FSC literature focuses on signals such as the one in Fig. 2a and to the best of the authors' knowledge the compression of CA signals has not been discussed yet. Furthermore, some FSC schemes that are based on resampling might not properly work when the intraband CA signal has frequencies close to the Nyquist frequency.

An alternative FSC method that does not rely on resampling

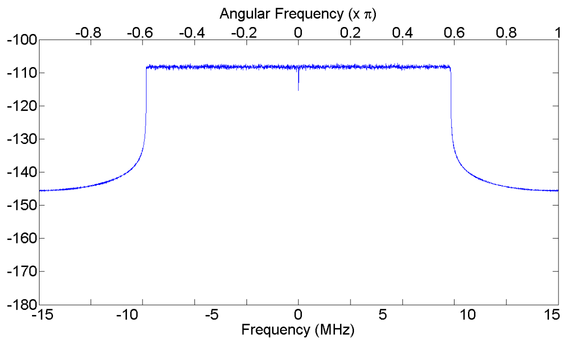

(a) Non-CA LTE signal with BW=20 MHz.

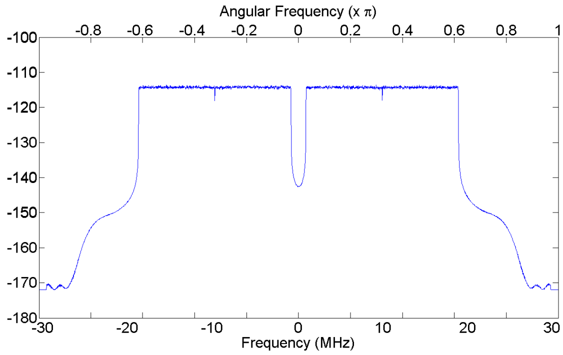

(b) Intraband CA signal with f_{c1}=-9.9 MHz, f_{c2}=9.9 MHz and OSR ≈1.63.

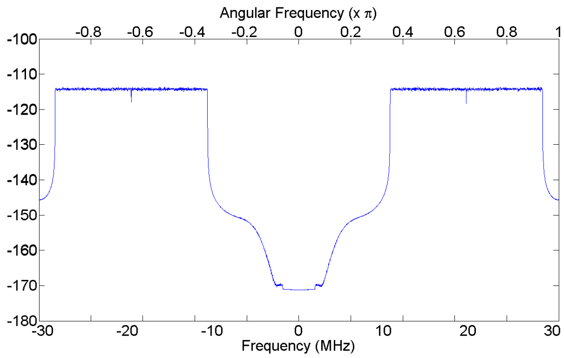

(c) Intraband CA signal with f_{c1}=-19.8 MHz, f_{c2}=19.8 MHz and OSR ≈1.07.

Fig. 2: Spectrum of an non-CA LTE signal (a) and scenarios for intraband CA signals in (b) and (c). The legacy LTE signal has BW of 20 MHz and it is sampled with F_s=30.72 MHz. The intraband CA signals sampled at F_s=61.44 MHz and havetwo CCs of 20 MHz spaced by 19.8 and 38.6 MHz.

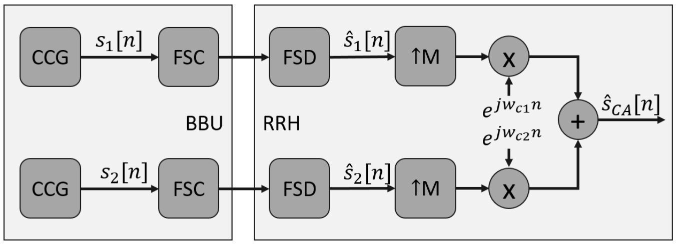

(a) Compression of each CC and the intraband CA signal is created at RRH.

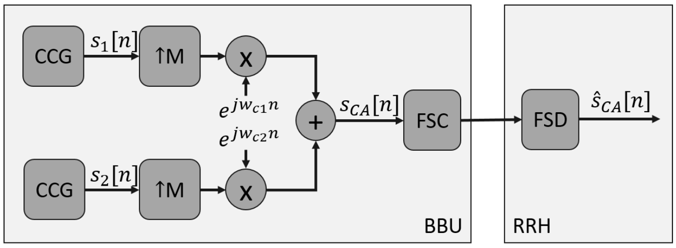

(b) Compression of intraband CA signal.

Fig. 3: Options for FSC of intraband CA signals.

is the scheme proposed by the authors in [3], which uses an OFDM-adapted linear predictive coding (LPC) in combination with lossless Huffman coding. The main advantage of this method over the one based on resampling is that it does not depend on the position of CCs in the spectrum of the signal being compressed. Thus, the method in [3] could be used in both compression scenarios of Fig. 3, as shown by the simulation results in the next section. Note that in [3] the authors show results only for non-CA LTE signal such as the one in Fig. 2a. Here, extra results are provided, exploiting different scenarios of CA signals and signal compression.

III. Simulation Results

The two compression scenarios of Fig. 3 were simulated and the results were compared in terms of average error vector magnitude (EVM) and compression factor (F), which are common figure of merits used in FSC schemes [3]–[7]. The average EVM was calculated as specified in [15, Annex E] and the compression factor is the ratio between the original and compressed signal sizes.

In Fig. 3a, each component carrier is compressed independently and the CA signal is constructed after decompression, at RRH. Additionally, Fig. 3b shows other scenario where the CA signal is constructed in the BBU and then compressed, before transmission of the CA signal over the fronthaul.

One goal of the simulations is to compare which option in Fig. 3 is better for compression of CA signals. In other words, this objective is to compare what is more effective: to compress each component carrier individually or the aggregated signal. Since some FSC schemes that are based on resampling might not properly work in some CA scenarios, the simulations were performed with the FSC method proposed in [3] that is not based on resampling.

Three simulations were performed, called Scenario 1, Scenario 2 and Scenario 3. In Scenario 1, the compression is executed as depicted in Fig. 3a, where two LTE signals are created at BBU, compressed and the intraband CA signal is created, at RRH. Scenario 2 and Scenario 3 use the architecture of Fig. 3b with signals similar to Fig. 2b and Fig. 2c, respectively. That is, Scenario 2 and 3 evaluate the impact of the component carrier position in the FSC scheme of [3]. In all scenarios, the EVM is calculated from the signal $\hat{s}_{\mathrm{CA}}[n]$, i. e., after aggregating the CA signal and the decompression.

The method proposed in [3] requires a training signal to create a prediction filter, quantizer and Huffman dictionary. In the present paper, 10 LTE frames were used to train these three components of the FSC scheme. In Scenario 1, the training signal is a non-CA LTE signal, since the CA signal

TABLE I: Compression of each CC and CA generation at RRH (Scenario 1).

	10 MHz		20 MHz	
Modulation	EVM (%)	F	EVM (%)	F
QPSK	1.15	3.32	1.22	3.42
16-QAM	1.18	3.36	1.21	3.41
64-QAM	1.19	3.56	1.21	3.41

TABLE II: Compression results of CA signals with OSR=1.63 (Scenario 2).

	10 MHz		20 MHz	
Modulation	EVM (%)	F	EVM (%)	F
QPSK	1.76	3.59	1.83	3.68
16-QAM	1.78	3.60	1.88	3.71
64-QAM	1.76	3.59	1.80	3.66

TABLE III: Compression results of CA signals with OSR=1.07 (Scenario 3).

	10 MHz		20 MHz	
Modulation	EVM (%)	F	EVM (%)	F
QPSK	2.05	3.61	1.82	3.52
16-QAM	1.91	3.53	2.07	3.65
64-QAM	2.15	3.66	1.88	3.55

is created only after decompression. In the other cases, in Scenarios 2 and 3 the training signal is a intraband CA signal composed of two component carriers. In all scenarios the FSC method was configured with a quantizer of 6 bits and a sixth order predictor.

After training, the results of all scenarios were captured by simulating 30 LTE frames for each component carrier configured as 10 and 20 MHz LTE signals. In all cases, the modulation of the LTE signals was tested with QPSK, 16-QAM and 64-QAM, which require a maximum EVM of 17.5, 12.5 and 8%, respectively [15].

The results of Scenario 1 are shown in Table I where the EVM and compression factor are approximately 1.2% and 3.4 in both cases of bandwidth. This shows that the performance of the FSC scheme [3] does not varies with the bandwidth when used as depicted in Fig 3a. In fact, the FSC scheme [3] performance does not vary significantly with the modulation and bandwidth, but here it is shown that the compression combined with the carrier aggregation also does not impact the performance.

The results of Scenario 2 and 3 are shown in Tables II and Table III, respectively. In both cases the EVM was between 1.7 and 2.1% which is well below the required EVM for 256-QAM, as specified by 3GPP [15]. Furthermore, the performance of [3] does not have large variations with the position of the component carriers on spectrum, as shown by EVM and by the compression factor which varies only between 3.5 and 3.7 in these scenarios.

In summary, for the Scenarios 2 and 3 the differences in EVM and compression factor are less than 0.4% and less than 0.2, respectively. These differences are negligible and show that the method in [3] could compress the signal regardless of the position of the component carriers. Furthermore, the results of all scenarios (1 to 3) shows that the method in [3] could be effective in reducing the volume of data in both cases of Fig. 3. The compression in Scenario 1 gives lower EVM and lower compression factor than in Scenarios 2 and 3, i. e., with the method of [3], the compression of each CC independently gives a slightly lower distortion than compressing the CA signal at the cost of lightly reduced compression factor. Moreover, Scenario 1 have a higher computational cost at the RRH due to the CA generation, while in Scenarios 2 and 3 the RRH only has the computational cost of the decompression.

IV. Conclusions

This work introduced some aspects of carrier aggregation signals that are relevant for fronthaul signal compression schemes. Many methods in literature are based on resampling and might have low performance depending on the position of the component carriers.

The method in [3] does not use resampling in its implementation and was evaluated for different compression scenarios. It can compress CA signals with no modifications on the method. Furthermore, it can compress CA signals independently of the placement of the CCs, while the resampling methods cannot compress CA signals with CCs next to the Nyquist frequency.

In carrier aggregation, the designer might have the option of compressing each CC independently, and then aggregating them at the RRH. It was shown that this approach also leads to relatively low distortions. Furthermore, it can also work with many of the available FSC schemes, since the signal that must be compressed is similar to legacy LTE signals. On the other hand, compressing the CCs together may reduce the processing at the RRH, by making the CA generation in the BBU.

References

[1] A. Checko, H. Christiansen, Y. Yan, L. Scolari, G. Kardaras, M. Berger, and L. Dittmann, "Cloud RAN for Mobile Networks - A Technology Overview," *IEEE Communications Surveys Tutorials*, vol. 17, no. 1, pp. 405–426, Firstquarter, 2015.

[2] D. Wubben, P. Rost, J. S. Bartelt, M. Lalam, V. Savin, M. Gorgoglione, A. Dekorsy, and G. Fettweis, "Benefits and Impact of Cloud Computing on 5G Signal Processing: Flexible centralization through cloud-RAN," *IEEE Signal Processing Magazine*, vol. 31, no. 6, pp. 35–44, Nov 2014.

[3] L. Ramalho, M. N. Fonseca, A. Klautau, C. Lu, M. Berg, E. Trojer, and S. Höst, "An LPC-Based Fronthaul Compression Scheme," *IEEE Communications Letters*, vol. 21, no. 2, pp. 318–321, Feb 2017.

[4] H. Si, B. L. Ng, M. S. Rahman, and J. Zhang, "A Novel and Efficient Vector Quantization Based CPRI Compression Algorithm," *CoRR*, 2015. [Online]. Available: http://arxiv.org/abs/1510.04940.

[5] B. Guo, W. Cao, A. Tao, and D. Samardzija, "LTE/LTE-A Signal Compression on the CPRI Interface," *Bell Labs Technical Journal*, vol. 18, no. 2, pp. 117–133, Sept 2013.

[6] D. Samardzija, J. Pastalan, M. MacDonald, S. Walker, and R. Valenzuela, "Compressed Transport of Baseband Signals in Radio Access Networks," *Wireless Communications, IEEE Transactions on*, vol. 11, no. 9, pp. 3216–3225, September 2012.

[7] K. Nieman and B. Evans, "Time-domain Compression of Complex-Baseband LTE Signals for Cloud Radio Access Networks," in *Global Conference on Signal and Information Processing (GlobalSIP), 2013 IEEE*, Dec 2013, pp. 1198–1201.

[8] M. Iwamura, K. Etemad, M. h. Fong, R. Nory, and R. Love, "Carrier Aggregation Framework in 3GPP LTE-Advanced," *IEEE Communications Magazine*, vol. 48, no. 8, pp. 60–67, August 2010.

[9] G. Ku and J. M. Walsh, "Resource Allocation and Link Adaptation in LTE and LTE Advanced: A Tutorial," *IEEE Communications Surveys Tutorials*, vol. 17, no. 3, pp. 1605–1633, thirdquarter 2015.

[10] G. Yuan, X. Zhang, W. Wang, and Y. Yang, "Carrier Aggregation for LTE-Advanced Mobile Communication Systems," *IEEE Communications Magazine*, vol. 48, no. 2, pp. 88–93, February 2010.

[11] R. Ratasuk, D. Tolli, and A. Ghosh, "Carrier Aggregation in LTE-Advanced," in *Vehicular Technology Conference (VTC 2010-Spring), 2010 IEEE 71st*, May 2010, pp. 1–5.

[12] K. I. Pedersen, F. Frederiksen, C. Rosa, H. Nguyen, L. G. U. Garcia, and Y. Wang, "Carrier Aggregation for LTE-Advanced: Functionality and Performance Aspects," *IEEE Communications Magazine*, vol. 49, no. 6, pp. 89–95, June 2011.

[13] S. A. Bassam, W. Chen, M. Helaoui, and F. M. Ghannouchi, "Transmitter Architecture for CA: Carrier Aggregation in LTE-Advanced Systems," *IEEE Microwave Magazine*, vol. 14, no. 5, pp. 78–86, July 2013.

[14] Z. Shen, A. Papasakellariou, J. Montojo, D. Gerstenberger, and F. Xu, "Overview of 3GPP LTE-Advanced Carrier Aggregation for 4G Wireless Communications," *IEEE Communications Magazine*, vol. 50, no. 2, pp. 122–130, February 2012.

[15] 3GPP TS 36.104, "Evolved Universal Terrestrial Radio Access (E-UTRA); Base Station (BS) Radio Transmission and Reception," 2014. [Online]. Available: http://www.3gpp.org/dynareport/36104.htm